Synthetic prions generated in vitro are similar to a newly identified subpopulation of PrPSc from sporadic Creutzfeldt-Jakob disease

Synthetic prions generated in vitro are similar to a newly identified subpopulation of PrP^{Sc} from sporadic Creutzfeldt-Jakob Disease

OLGA V. BOCHAROVA,[1] LEONID BREYDO,[1] VADIM V. SALNIKOV,[1] ANDREW C. GILL,[3] AND ILIA V. BASKAKOV[1,2]

[1]Medical Biotechnology Center, University of Maryland Biotechnology Institute, Baltimore, Maryland 21201, USA
[2]Department of Biochemistry and Molecular Biology, University of Maryland School of Medicine, Baltimore, Maryland 21201, USA
[3]Institute for Animal Health, Compton, Newbury, Berkshire, RG20 7NN, United Kingdom

(RECEIVED October 20, 2004; FINAL REVISION January 17, 2005; ACCEPTED January 23, 2005)

Abstract

In recent studies, the amyloid form of recombinant prion protein (PrP) encompassing residues 89–230 (rPrP 89-230) produced in vitro induced transmissible prion disease in mice. These studies showed that unlike "classical" PrP^{Sc} produced in vivo, the amyloid fibrils generated in vitro were more proteinase-K sensitive. Here we demonstrate that the amyloid form contains a proteinase K-resistant core composed only of residues 152/153–230 and 162–230. The PK-resistant fragments of the amyloid form are similar to those observed upon PK digestion of a minor subpopulation of PrP^{Sc} recently identified in patients with sporadic Creutzfeldt-Jakob disease (CJD). Remarkably, this core is sufficient for self-propagating activity in vitro and preserves a β-sheet-rich fibrillar structure. Full-length recombinant PrP 23-230, however, generates two subpopulations of amyloid in vitro: One is similar to the minor subpopulation of PrP^{Sc}, and the other to classical PrP^{Sc}. Since no cellular factors or templates were used for generation of the amyloid fibrils in vitro, we speculate that formation of the subpopulation of PrP^{Sc} with a short PK-resistant C-terminal region reflects an intrinsic property of PrP rather than the influence of cellular environments and/or cofactors. Our work significantly increases our understanding of the biochemical nature of prion infectious agents and provides a fundamental insight into the mechanisms of prions biogenesis.

Keywords: prion protein; amyloid fibrils; conformational transition; proteinase K; Creutzfeldt-Jakob disease

Several severe neurodegenerative diseases including Creutzfeldt-Jakob disease (CJD), Gerstmann-Straussler-Sheinker disease, and fatal familial insomnia are associated with misfolding and aggregation of the prion protein (Prusiner 2001). Prion maladies manifest themselves in infectious, familial, and sporadic forms. To explain the infectious form of the prion diseases, the "protein-only hypothesis" postulates that an abnormal isoform of the prion protein, PrP^{Sc}, acts as an infectious agent and propagates its pathological conformation in an autocatalytic manner using the normal isoform of the same protein, PrP^{C}, as a substrate (Prusiner 1982).

PrP^{C} and PrP^{Sc} differ substantially in their conformations. Unlike PrP^{C}, PrP^{Sc} is a multimeric assembly characterized by enhanced resistance to proteinase K (PK) digestion and by an increase in the amount of β-sheet structure

Reprint requests to: Ilia V. Baskakov, 725 W. Lombard Street, Baltimore, MD 21201, USA; e-mail: Baskakov@umbi.umd.edu; fax: (410) 706-8184.

Abbreviations: CJD, Creutzfeldt-Jakob disease; spCJD, sporadic CJD; PrP, prion protein; PrP^{C}, the normal, cellular isoform of PrP; PrP^{Sc}, the abnormal, infections isoform of PrP; rPrP, recombinant PrP; rPrP 89-230, recombinant PrP encompassing residues 89–230; rPrP 23-230, full-length recombinant PrP; α-rPrP 89-230, α-helical isoform of rPrP 89-231; α-rPrP 23-230, α-helical isoform of rPrP 23-231; PK, proteinase K; PrP 27-30, PK-resistant core of classical PrP^{Sc}; ThT, Thioflavin T; GdnHCl, guanidinium hydrochloride; FTIR; Fourier transform infrared spectroscopy.

Article and publication are at http://www.proteinscience.org/cgi/doi/10.1110/ps.041186605.

(Caughey et al. 1991; Pan et al. 1993). The detailed three-dimensional structure of the PrP^{C} isoform has been determined (Riek et al. 1996, 1997; Donne et al. 1997; Haire et al. 2004), whereas structural information about PrP^{Sc} is more limited due to its insolubility, heterogeneity, and highly aggregated state (Gabizon and Prusiner 1990; Wille et al. 2002).

In contrast to PrP^{C}, PrP^{Sc} exists in multiple conformations, which are believed to result from infection of animals with different *strains* of TSE (transmissible spongiform encephalopathy) agent. The existence of different prion strains has been recognized for many years (Dickinson et al. 1968; Fraser and Dickinson 1973), but has only recently been linked to the conformational diversity of PrP^{Sc}. According to the template-assisted model, each conformation of PrP^{Sc} can act as a unique template, providing conformational constraints for the formation of nascent PrP^{Sc} and, therefore, determining the conformation of nascent PrP^{Sc} (Cohen et al. 1994). Biochemical assays have been described that distinguish conformers of PrP^{Sc} by the extent of PK resistance, the size of the PK-resistant core, thermodynamic stability, epitope presentation, and relative amount of β-sheet-rich structure (Bessen and Marsh 1994; Telling et al. 1996; Caughey et al. 1998; Safar et al. 1998; Peretz et al. 2001). Conformationally different subtypes of PrP^{Sc} have also been found in patients with sporadic CJD (spCJD) (Parchi et al. 1999; Hill et al. 2003). These PrP^{Sc} *subtypes* have variations in the molecular mass of the PK-resistant core and exhibit different ratios of di-, mono-, and unglycosylated PrP^{Sc}. Conformational diversity of PrP^{Sc} subtypes is linked to the methionine/valine polymorphism at codon 129 and may also be affected by unidentified host factors (Telling et al. 1995; Parchi et al. 2000).

To distinguish different conformers and to classify subtypes of PrP^{Sc}, limited digestion with PK has been used widely since it offers a rapid and accurate assay of altered PrP^{Sc} conformation (McKinley et al. 1983; Bessen and Marsh 1994; Safar et al. 1998; Parchi et al. 1999; Hill et al. 2003). Normally, treatment of PrP^{Sc} with PK generates a C-terminal PK-resistant core, referred to as PrP 27-30 (McKinley et al. 1983; Oesch et al. 1985). Depending on the subtype of PrP^{Sc}, PrP 27-30 exhibits minor variations in gel mobility due to differences in the PK cleavage site between residues 79 and 103 (Parchi et al. 2000). In addition, two novel PK-resistant fragments were identified recently in patients with spCJD (Zou et al. 2003). Deglycosylated forms of these novel PK-resistant fragments migrate at 13 and 12 kDa by SDS-PAGE, and are generated by cleavage at residues 154/156 and 162/167, respectively, retaining the C-terminal region intact (Zou et al. 2003). Multiple factors including gene polymorphism, glycosylation, and as yet unidentified cellular factors may contribute to the broad conformational diversity of PrP^{Sc}. It is therefore important to know whether this conformational diversity reflects an intrinsic property of PrP or arises only with assistance from other molecules in a cell. Is unglycosylated recombinant PrP (rPrP) capable of mimicking any known PrP^{Sc} subtypes in the absence of the cellular environment or templating?

To address this question we investigated the amyloid form of mouse (Mo) rPrP spanning residues 89–230 (rPrP 89-230) by use of limited proteolysis with PK. In our previous studies, we showed that in vitro conversion of rPrP to the amyloid form in the absence of the cellular environment exhibited peculiar features of the autocatalytic process and was limited by a species barrier, two key aspects of prion propagation (Baskakov 2004). Furthermore, we demonstrated that the amyloid form of Mo rPrP 89-230 generated in vitro induces a transmissible form of prion disease in transgenic mice expressing mouse PrP 89-230 (Baskakov et al. 2002; Legname et al. 2004). Long incubation times observed upon inoculation of the amyloid fibrils suggest that the fibrils generated in vitro have very low infectivity titers. However, shortening of the incubation times observed in the subsequent passages of the synthetic prions in transgenic and wild-type mice allows an alternative explanation. One may speculate that the synthetic prions undergo adaptation upon propagation in vivo, and that the differences in the incubation time are attributed to an apparent transmission barrier. Consistent with this hypothesis are several lines of evidence including biochemical and neuropathological features that indicate that the synthetic prions induced a novel strain of prion disease in experimental animals. Encouraged by these findings, we wished to determine whether the amyloid fibrils, produced in vitro without other cellular components or PrP^{Sc}-templating, structurally resembled any known isoforms or subtypes of PrP^{Sc}.

Here we demonstrate that that the amyloid fibrils closely resemble the novel subpopulation of PrP^{Sc} associated with spCJD. Using PK digestion we identified three major PK-resistant fragments in the amyloid form. These fragments migrated at about 12 kDa, 10 kDa, and 8 kDa by SDS-PAGE and encompassed residues 138/141–230, 152/153–230, and 162–230, respectively, as determined by mass spectrometry. This suggests that the slow propagation rate observed in the first passage and an apparent transmission barrier are due to a proteolytically labile region encompassing residues 89–138. Remarkably, upon digestion with PK, short C-terminal fragments remained assembled in fibrillar structures, maintained high β-sheet content, and preserved their seeding activity. Since no cellular factors and templates were used to generate the amyloid form in vitro, we suggest that the formation of the novel subpopulation of PrP^{Sc} with this particular PK-resistant core reflects an intrinsic property of PrP.

Results and Discussion

It is well established that PrP^{Sc} is highly resistant toward denaturation and remains infectious even in extreme dena-

turing conditions (Prusiner et al. 1993). Conversely, the thermodynamic stability of PrP^C is modest and comparable to that of other globular proteins (Baskakov et al. 2001). To test whether the amyloid conformation of rPrP 89-230 possesses increased thermodynamic stability, we investigated guanidinium hydrochloride (GdnHCl)-induced denaturation at various temperatures. The amyloid form of Mo rPrP 89-230 was produced in vitro as described (Baskakov et al. 2002). At 24°C, $C_{1/2}$ (the concentration of GdnHCl at the midpoint of denaturation) of GdnHCl-induced denaturation of the amyloid fibrils was 4.2 M, while increasing the temperature to 57°C decreased $C_{1/2}$ to 3.1 M (Fig. 1). These results demonstrate that either high concentrations of GdnHCl or increased temperatures and intermediate GdnHCl concentrations are required for denaturation of amyloid form. In contrast, α-monomeric form of rPrP can be denatured by moderate concentrations of GdnHCl ($C_{1/2}$ = 2.2 M at room temperature) (Swietnicki et al. 1998). Remarkably, the $C_{1/2}$ value for denaturation of amyloid fibrils generated in vitro (4.2 M) was identical to the $C_{1/2}$ value determined for the mouse synthetic prion strain 1 (MoSP1) produced in the brains of Tg9949 mice after inoculation of amyloid fibrils (Legname et al. 2005). Increased resistance toward denaturation is consistent with the formation of a larger solvent-protected core during the transition from monomer into amyloid conformation.

To distinguish different subtypes of PrP^{Sc}, limited digestion with PK has been used widely, since it offers a rapid and accurate assay of altered PrP^{Sc} conformation (McKinley et al. 1983; Bessen and Marsh 1994; Safar et al. 1998; Parchi et al. 1999; Hill et al. 2003; Notari et al. 2004). In our previous study we failed to identify any PK-resistant polypeptides upon digestion of the amyloid fibrils using standard conditions for SDS-PAGE (Baskakov et al. 2002). In the present study we found that PK-resistant polypeptides can be detected by SDS-PAGE, but only when, in addition to SDS-sample buffer, urea is added to the sample buffer to a final concentration of 3 M. After PK digestion we observed three major fragments having apparent molecular masses of 12 kDa, 10 kDa, and 8 kDa (Fig. 2A, left panel). As the PK to protein ratio increased, the size of PK-resistant polypeptides was reduced. Thus, digestion at 1:2000 PK/rPrP ratio produced primarily fragments with apparent molecular masses of 12 kDa and 10 kDa (lane 2), while at a higher ratio (up to 1:20) the major PK-resistant fragments were 10-kDa and 8-kDa peptide (lane 5). The PK/rPrP ratio of 1:20 exceeds the PK-to-protein ratios that are normally used in studies of PrP^{Sc} in brain homogenates (Caughey et al. 1998; Safar et al. 1998). Moreover, our PK digestion assay is free from nonprotein components of brain homogenate and from possible interference with PK activity. It is noteworthy that when SDS-sample buffer was not supplemented with urea, we observed stalled bands on the top of the stacking gel instead of 10-kDa and 8-kDa bands. Because treatment under highly denatured conditions, including 3M urea, 2% SDS, and 95°C was necessary for analyses of proteolytic products by SDS-PAGE, it is likely that the PK-resistant core of the amyloid form remained assembled in a highly stable, multimeric form.

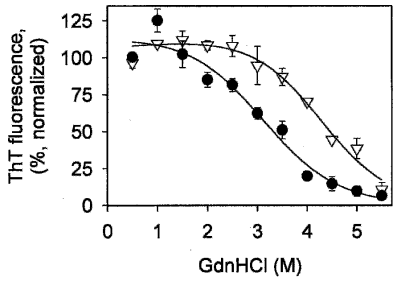

Figure 1. GdnHCl-induced denaturation of the amyloid fibrils of rPrP 89-230. Amyloid fibrils were incubated for 30 min at 24°C (▽) or 57°C (●) in the presence of variable concentrations of GdnHCl. The GdnHCl concentration was then adjusted to 0.55 M, followed by a ThT-binding assay. The experiments were conducted at least in duplicate. The lines represent the results of the fitting to a two-state model (Santoro and Bolen 1988). The increase in ThT fluorescence observed at low concentrations of denaturant is due to GdnHCl-induced dissociation of coaggregated amyloid fibrils.

To ensure that the PK-resistant fragments are not generated from cleavage of residual amounts of α-rPrP 89-230 that may copresent in the preparation of the amyloid fibrils, we treated α-rPrP 89-230 with PK using identical digestion conditions. At low concentrations of PK (PK/rPrP ratios 1:2000 and 1:500), α-rPrP 89-230 generated two major fragments having apparent molecular masses of 14 kDa and 13 kDa (Fig. 2A, middle panel, lanes 2,3, respectively). At higher concentrations of PK (PK/rPrP ratios 1:100 and 1:20), these fragments were completely digested (lanes 4,5, respectively). The result of this control experiment is consistent with previous studies that demonstrated that PrP^C undergoes proteolytic cleavage at amino acid residues 110/111 to produce a C-terminal fragment referred to as C1 (Chen et al. 1995). Taken together, our studies shows that 8-kDa and 10-kDa fragments are generated from the amyloid fibrils but not from α-rPrP 89-230.

To identify the region that is resistant to PK digestion in the amyloid conformation, we used Fabs P and R1, specific to residues 96–105 and 225–230, respectively. The epitope for Fab P was not present in any of the three major PK-resistant products, while the epitope for Fab R1 was present in all three fragments. Using liquid chromatography/mass spectrometry (LC-MS) we showed that the three major PK-resistant bands correspond to polypeptides spanning residues 138/141–230, 152/153–230, and 162–230 (Fig. 2B). Both LC-MS and Western blot analyses demonstrate that the C-terminal region of rPrP 89-230 remains PK-resistant in the amyloid form, while the central region encompassing residues 89–138 is fully susceptible to proteolysis (Fig. 3A).

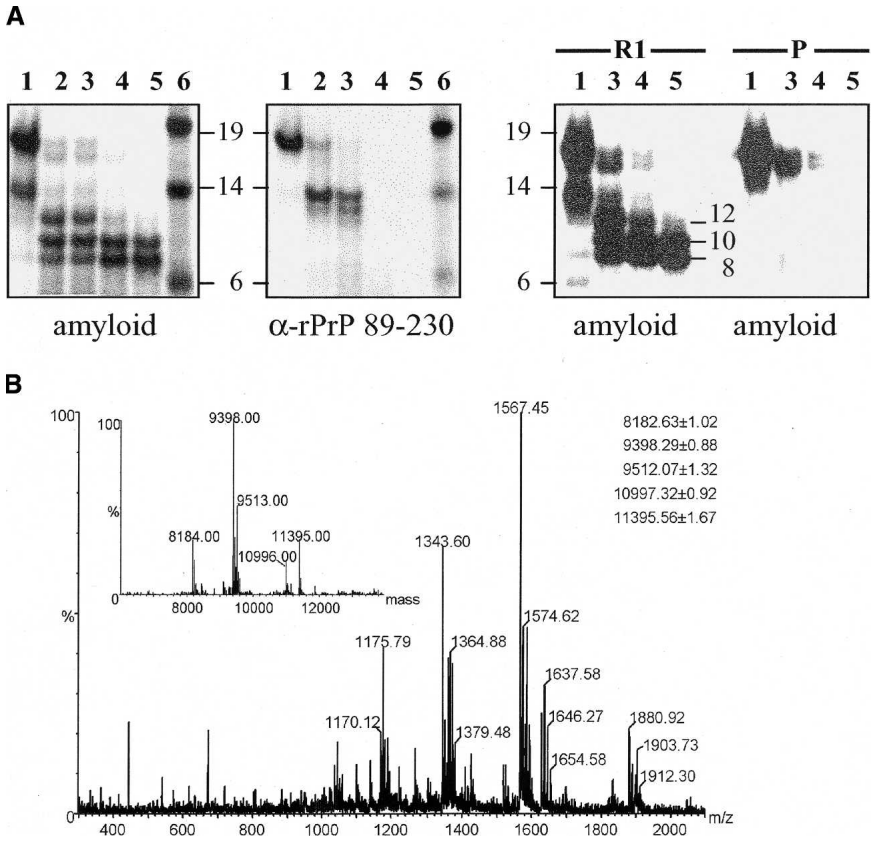

Figure 2. Limited PK digestion of the amyloid form of rPrP 89-230. (*A*) Amyloid fibrils or α-rPrP 89-230 (0.2 mg/mL) were treated with PK for 1 h at 37°C at the following PK:rPrP ratios (w/w): 1:2000 (lanes *2*), 1:500 (lanes *3*), 1:100 (lanes *4*), 1:20 (lanes *5*), no PK (lanes *1*) and analyzed by SDS-PAGE followed by silver staining (amyloid fibrils, *left* panel; α-rPrP 89-230, *middle* panel) or by Western blotting using Fabs R1 and P (*right* panel). MW markers, lane *6*. A 14-kDa fragment detectible by Fab R1 appeared as a result of partial degradation in the time-course of amyloid formation. (*B*) Online capillary HPLC-MS analysis of the amyloid form after limited digestion with PK. Electrospray mass spectrum and deconvoluted mass spectrum of species (*inset*) showing partial resistance to PK. Several PK-resistant species were identified by comparison of measured and theoretical masses, including polypeptides spanning residues 138–230 (measured mass 11,395.56 Da; theoretical mass 11,395.56 Da), residues 141–230 (measured mass 10,997.32 Da; theoretical mass 10,998.01 Da), residues 152–230 (measured mass 9,512.07 Da; theoretical mass 9,513.58 Da), residues 153–230 (measured mass 9,398.29 Da; theoretical mass 9,399.47 Da), and residues 162–230 (measured mass 8,182.63 Da; theoretical mass 8,184.07).

The 10-kDa and 8-kDa fragments produced at high PK/rPrP ratio were different from C1 fragment generated upon proteolytic digestion of PrP^{C} (Chen et al. 1995), but remarkably similar to a minor population of PK-resistant fragments of PrP^{Sc} identified recently in patients with spCJD (Fig. 3B;Zou et al. 2003). These fragments were found in 26 of the 29 spCJD brains examined and accounted for up to 24% of all PK-resistant PrP polypeptides in spCJD brains. Chen and coauthors suggested that these short C-terminal fragments were generated from a novel subpopulation of PrP^{Sc} that adopts a conformation different from that of "classical" PrP^{Sc} (Zou et al. 2003), which is known to produce a core encompassing residues ~90–230 upon PK digestion (for clarity, the minor subpopulation of PrP^{Sc} produced in spCJD will be referred to as novel PrP^{Sc}). Another group reported that C-terminal PK-resistant fragments of 11–12 kDa were also associated with a certain type of iatrogenic CJD; however, the exact positions of PK cleavage sites were not determined (Satoh et al. 2003). Truncated, PK-resistant C-terminal polypeptides of similar length were found in brain homogenate from mice infected with mouse-passaged hamster PrP^{Sc} strain 263K and in cell-free conversion assays under conditions that mimicked the hamster/mouse species barrier (Lawson et al. 2004). The sites of PK cleavage were found to be between residues 130 and 157 as localized by epitope mapping and mobility on a gel (Fig. 3C). Identification of novel C-terminal PK-resistant fragments in patients with sporadic and iatrogenic CJD as well as in mice suggested that their involvement in the pathogenic process may be more common than had previously been recognized (Satoh et al. 2003; Zou et al. 2003; Lawson et al. 2004). On the basis of limited proteolysis, the amyloid

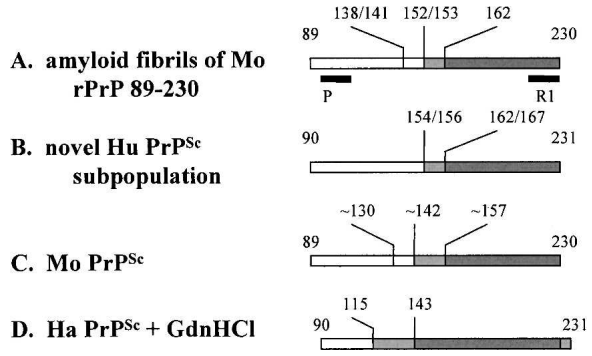

Figure 3. PK-resistant fragments. (*A*) PK-resistant core of the amyloid fibrils of Mo rPrP 89-231; epitopes for Fabs P and R1 are highlighted (present work). (*B*) PK-resistant core of the novel subpopulation of PrP^{Sc} found in spCJD; sites of PK digestion were identified by N-terminal sequencing using Edman degradation (Zou et al. 2003). (*C*) PK-resistant core of PrP^{Sc} generated in mice upon second passage of transmission of hamster PrP^{Sc} strain 263 K as determined by Western blotting using an antibody against the C terminus. Approximate sites of cleavage were identified by epitope mapping of PK-resistant fragments of Mo PrP generated in the cell-free conversion assay upon incubation with hamster PrP^{Sc} strain 263 K (Lawson et al. 2004). (*D*) PK-resistant core of hamster (Ha) PrP^{Sc} generated in the presence of 2.5 M GdnHCl. The approximate location of PK cleavage was found within residues 115–143 by epitope mapping, and is represented by the light gray area (Kocisko et al. 1996). PK-resistant regions are represented by the dark gray area, and partial PK-resistant regions by the light gray area.

form of rPrP 89-230 is similar to the novel rather than classical subpopulations of PrP^{Sc}.

Multiple lines of evidence indicate that the central region of PrP, encompassing residues 90–141, is important for prion propagation (Tagliavini et al. 1993; Fischer et al. 1996; Peretz et al. 1997; Chabry et al. 1998). Puzzled by the fact that this region is PK-labile in disease-producing amyloid fibrils and, therefore, expected to undergo rapid digestion by endogenous proteases upon inoculation (Yadavalli et al. 2004), we sought to determine whether the C-terminal PK-resistant core maintains β-sheet-rich structure and possesses self-propagating activity. To address these questions we seeded the in vitro conversion reaction with the amyloid form pretreated with PK. For this experiment we used experimental conditions at which spontaneous or nonseeded formation of the amyloid fibrils occurred only after a prolonged lag phase of 60 h (Table 1). Seeding of the in vitro reaction with fibrils not treated with PK substantially reduced the lag phase (Fig. 4A), and the data indicate a linear dependence between the length of the lag phase and the log[amount of seed] (Fig. 4B). Remarkably, the fibrils pretreated with PK for 1 h at 37°C showed substantial seeding activity. As judged from the length of the lag phase, 2.5% of amyloid fibrils pretreated with PK at 1:20 PK/rPrP ratio exhibited apparent seeding activities that were equivalent to the seeding activities that would be displayed by 0.75% of intact fibrils (Fig. 4A,B; Table 1). At a PK:rPrP ratio of

Table 1. *Kinetic parameters for amyloid formation*

	Lag-phase[a] (hours)
Nonseeded	59.8 ± 0.1
1% seed	18.5 ± 0.5
0.2% seed	22.4 ± 0.9
0.04% seed	27.6 ± 0.1
2.5% seed + PK[b]	19.9 ± 0.7

[a] The lag-phases were determined by fitting the time-dependent changes in the fluorescence of Thioflavin T vs. time of the reaction as described in Materials and Methods.
[b] The amyloid fibrils used for seeding were pretreated with PK for 1 h at 37°C at PK:rPrP ratio of 1:20.

1:20, only the 10-kDa and 8-kDa fragments, corresponding to residues 152/153–230 and 162–230, respectively, were detectable by Western blotting (Fig. 2A). This experiment illustrates that the C-terminal PK-resistant core of the synthetic prions preserves propagating activity in a cell-free conversion assay.

Since treatment under highly denaturing conditions was required for visualization of proteolytic products by SDS-PAGE, it is likely that the PK-resistant core of the amyloid fibrils remains assembled in a multimeric form. Therefore, we sought to determine whether the C-terminal PK-resistant core maintained fibrillar structure. Using electron microscopy we found that the amyloid form maintained fibrillar structure upon cleavage of N-terminal region (Fig. 5A). PK-treated fibrils had a higher tendency to coaggregate, probably due to an increase in accessibility of hydrophobic surfaces to the solvent upon PK digestion. Unfortunately, ag-

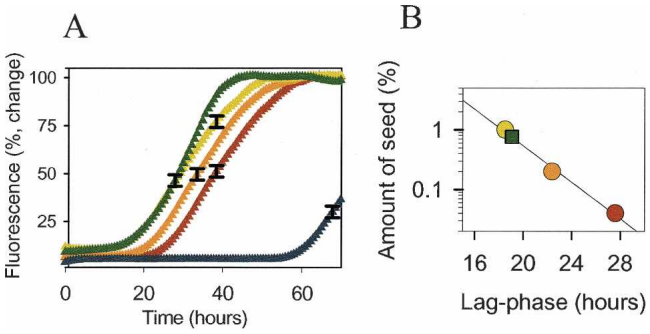

Figure 4. PK-resistant core of the amyloid form displays seeding activity. (*A*) The kinetics of fibril formation for rPrP 89-230 (0.3 mg/mL; reaction volume 0.15 mL) seeded with 0.04% (w/w) (brown triangles), 0.2% (orange triangles), and 1% (yellow triangles) of preformed fibrils; with 2.5% fibrils treated with PK (green triangles); and in nonseeded reaction (blue triangles). Std. dev. for duplicate samples are represented by error bars. The kinetics were monitored using the automated format as described in Materials and Methods. (*B*) Dependence of the lag phase of fibrils formation on the amount of seed (circles); the solid line represents the result of the fitting to a linear function. The apparent seeding activity in the reactions seeded with 2.5% of fibrils pretreated with PK at PK/rPrP ratio of 1:20 (green square) was calculated using the linear dependence between the length of the lag phase and Lg[amount of seed].

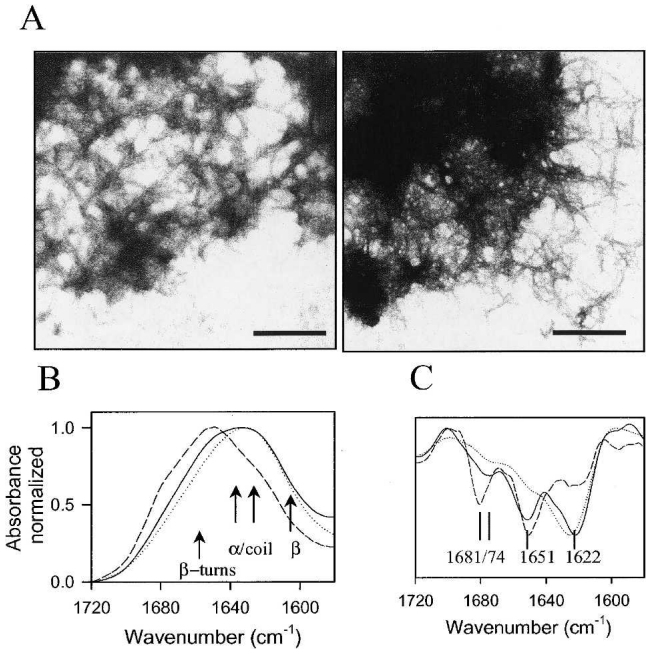

Figure 5. PK-resistant core of the amyloid form maintains β-rich structure. (*A*) Electron micrographs of the amyloid fibrils of rPrP 89-230 without PK treatment (*left* panel), and treated with PK at 37°C for 1 h at the PK to rPrP ratio of 1:20 (*right*). Scale bar = 0.5 μm. (*B*) FTIR spectra of rPrP 89-230 in the α-monomeric form (dashed line), the intact amyloid form (solid line), and the amyloid form after treatment with PK (dotted line). (*C*) Second derivatives of FTIR spectra. The line definitions are the same as for panel *B*. Fibrils were incubated with PK for 1 h at 37°C at the PK:rPrP ratio 1:20.

gregation of PK-treated fibrils into large clumps hampered quantitative analyses of the fibril width.

To test the extent to which PK digestion causes conformational changes in fibril secondary structure, we employed Fourier transform infrared spectroscopy (FTIR) using a Bio-ATR cell, which allows FTIR spectra to be recorded from aqueous solution. The FTIR spectrum acquired for α-rPrP 89-230 was dominated by strong absorbance at 1651 cm^{-1} and 1645 cm^{-1} corresponding to α-helices and random coil, respectively (Fig. 5B). The FTIR spectrum of the amyloid form was substantially different from that of the α-monomer. The second derivative analysis of the amyloid form revealed a major band at 1622 cm^{-1}, characteristic of β-sheet structures with strong intermolecular hydrogen bonds, a smaller band at 1651 cm^{-1}, indicative of α-helices and random coil, and a minor band at 1674 cm^{-1}, characteristic of β-turns and loops (Fig. 5C). Upon treatment with PK, the relative intensity of bands at 1651 cm^{-1} and 1674 cm^{-1} decreased, demonstrating loss of α-helical structure and β-turns and loops, respectively. The relative intensity of band at 1622 cm^{-1}, a characteristic of β-sheet structures, did not change notably. On the other hand, the shift of the band centered at 1622 cm^{-1} to 1626 cm^{-1} indicated that β-structures with strong intermolecular hydrogen bonds acquired some flexibility upon treatment with PK.

Since no cellular factors or templates were used for generation of the amyloid fibrils in vitro, the ability of rPrP 89-230 to adopt a conformation similar to that of novel PrP^{Sc} reflects an intrinsic property of PrP that is independent of the influence of cellular environments and/or cofactors. While the N-terminal region of PrP, encompassing residues 23–90, is not critical for transmission of prions, this region is known to influence the conformation of protease-resistant PrP isoforms (Wadsworth et al. 1999; Lawson et al. 2004), and may substantially impact the conformational diversity of fibrils generated in vitro. Therefore, we examined the conformation of the amyloid form generated from murine full-length recombinant PrP (rPrP 23-230).

Conversion of rPrP 23-230 to the amyloid fibrils was carried out using the same solvent conditions as those used for the conversion of rPrP 89-230. FTIR analysis of rPrP 23-230 refolded into the amyloid form produced a spectrum substantially different from that of the corresponding α-monomer (Fig. 6A). The spectrum of the amyloid form showed a substantial decrease in intensity of the band at 1654 cm^{-1} corresponding to α-helices and random coil, and an increase in intensity of the band at 1617 cm^{-1}, an indication of β-structure with strong intermolecular hydrogen bonds (Fig. 6B).

Analysis of PK-resistant fragments of the amyloid form of rPrP 23-230 showed two distinct patterns of cleavage, suggesting distinct subpopulations of conformers (Fig. 7A, left panel). The major subpopulation of rPrP 23-230 produces PK-resistant fragments of 12 kDa, 10 kDa, and 8 kDa similar to those identified from the PK digest of the amyloid

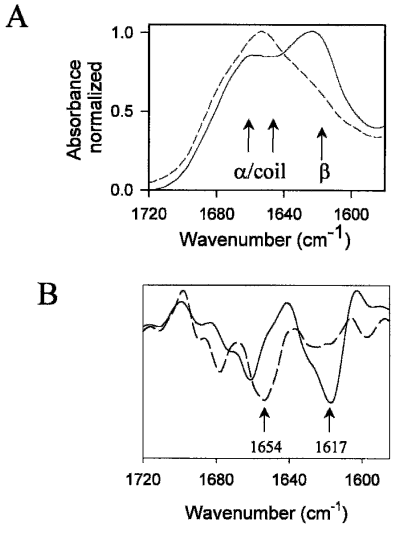

Figure 6. In vitro conversion of rPrP 23-230 into the amyloid fibrils. (*A*) FTIR spectra of rPrP 23-230 in the amyloid form (solid line) and in α-monomeric form (dashed line). (*B*) Second derivatives of FTIR spectra. The line definitions are the same as for panel *A*.

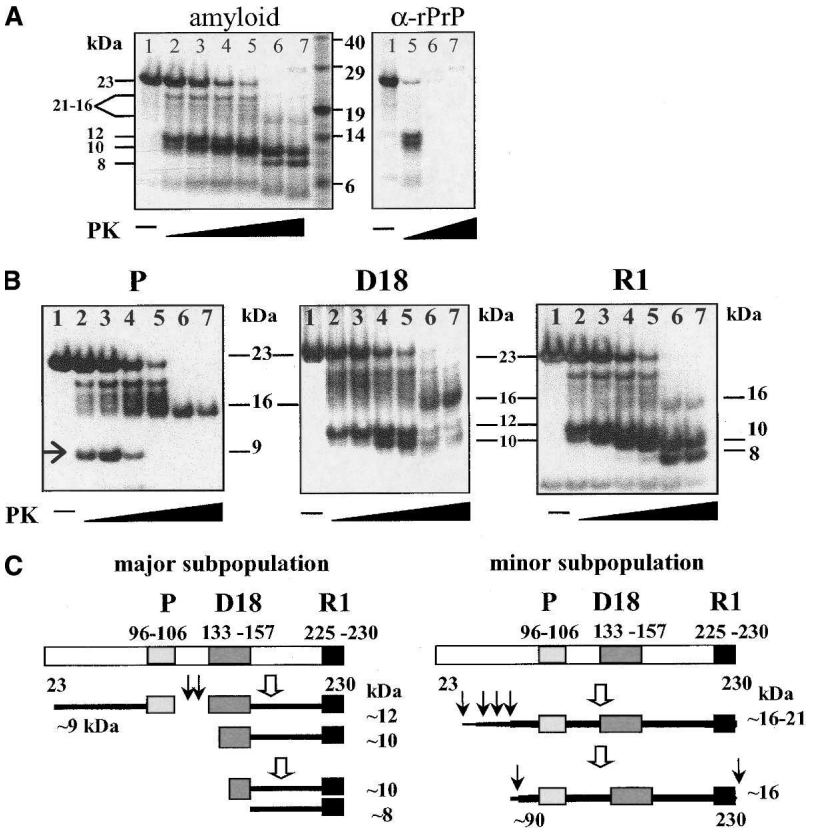

Figure 7. Limited PK digestion of the amyloid form of rPrP 23-230 reveals two conformers. (*A*) SDS-PAGE followed by silver staining represents the relative amount of PK-resistant fragments. Amyloid fibrils of rPrP 23-230 (*left* panel) or α-rPrP 23-230 (0.2 mg/mL) (*right*) were treated with PK for 1 h at 37°C at the following PK:rPrP ratios (w/w): no PK (lanes *1*), 1:10,000 (lanes *2*), 1:5,000 (lanes *3*), 1:1000 (lanes *4*), 1:500 (lanes *5*), 1:100 (lanes *6*), and 1:50 (lanes *7*). Apparent molecular masses of fragments are given in kDa at the *left*. (*B*) Western blot of the PK-resistant fragments treated with three Fabs: P (*left* panel), D18 (*middle*), and R1 (*right*). PK:rPrP ratios are the same as in panel *A*. The 9-kDa fragment containing epitope for Fab P appeared only at low PK:rPrP ratios (shown by an arrow). This fragment, however, was fully digested at high concentrations of PK. (*C*) Two patterns of PK digestion. Epitopes for Fab P are shown as light gray boxes, for D18 as dark gray boxes, and for R1 as black boxes; approximate locations of PK cleavage sites are shown by small arrows.

of rPrP 89-230. These fragments appear at low concentrations of PK and show the same pattern of epitope presentation as proteolytic fragments of the amyloid of rPrP 89-230 (Fig. 7B, left, middle, and right panels). The minor subfraction of rPrP 23-230, however, produces several bands with molecular masses between 21 and 16 kDa. These bands account for ~5%–10% of all PK-resistant products, as judged by SDS-PAGE (Fig. 7A, left panel). At PK:rPrP ratios of 1:100 and 1:50, these bands are further digested to generate a single PK-resistant product with molecular mass of 16 kDa (Fig. 7A, left panel, lanes 6,7). The 16-kDa fragment is consistently resistant to PK even upon incubation at the PK:rPrP ratio of 1:10 at 37°C for 1 h. This polypeptide contains epitopes for Fab P (residues 96–105), Fab D18 (residues 133–157), and Fab R1 (residues 225–230) (Fig. 7B). As a control to confirm that 8-kDa, 10-kDa, and 16-kDa PK-resistant fragments are generated from the amyloid fibrils, we used α-rPrP 23-230. At PK/rPrP ratios of 1:100 and 1:50, α-rPrP 23-230 was completely digested with no PK-resistant fragments being detected (Fig. 7A, left panel, lanes 6,7).

In parallel with limited PK digestion, two distinct subpopulations of the amyloid fibrils were evident by use of fluorescence and electron microscopy (Fig. 8). The majority of fibrils display relatively weak Thioflavin T (ThT)-fluorescence as seen by fluorescence microscopy (Fig. 8A). A minor subpopulation of fibrils (5%–10%), however, exhibits substantially brighter emission, which remains stable even after harsh PK treatment (Fig. 8A). This result is consistent with the two conformers identified by limited digestion in Figure 6. Two subpopulations of the fibrils were also seen by electron microscopy, where the minor subpopulation accounted for ~5% of all fibrils (Fig. 8B).

The results of limited proteolysis show that, upon conversion of rPrP 23-230 into the amyloid form, two subpopulations of conformers are generated, which differ in their

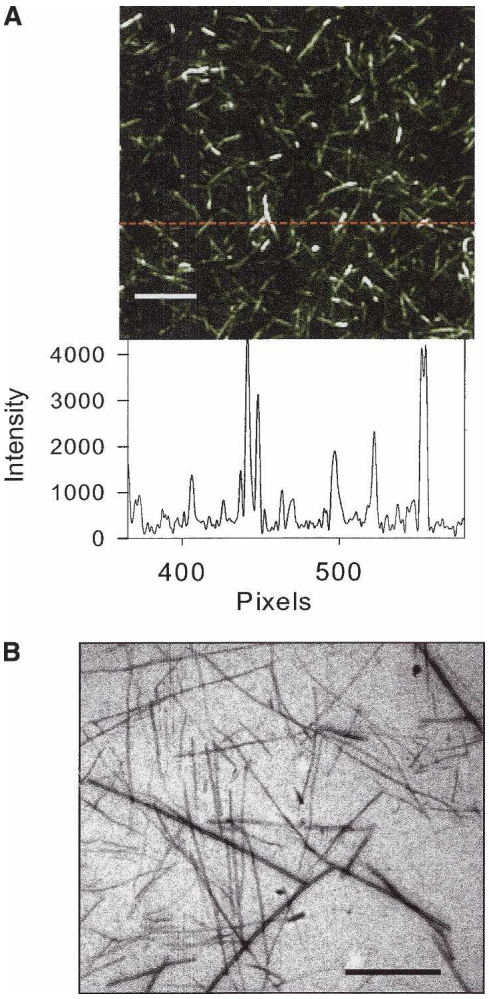

Figure 8. Two subpopulations of the amyloid fibrils of rPrP 23-230. (*A*) Fluorescence microscopy of the amyloid fibrils (*top* panel). The emission intensity (*bottom* panel) monitored across the image at the position shown by the red dashed line. The fibrils of minor subpopulations display emission intensities four-–eightfold higher than that of fibrils of the major subpopulation (scale bar = 2 μm). (*B*) Electron micrographs of negatively stained fibrils (scale bar = 0.5 μm). The minor subpopulation displayed much stronger propensity for staining with uranyl acetate and accounted for ~5%–10% of all fibrils.

resistance to PK (Fig. 7C). The major subpopulation is more sensitive to PK digestion and produces short C-terminal PK-resistant fragments similar to those generated from novel PrP^{Sc}. The minor subpopulation is characterized by enhanced resistance to PK and possesses a C-terminal resistant core identical to the PK-resistant fragments of classical PrP^{Sc}.

It is notable that conformers biochemically identical to both novel and classical PrP^{Sc} can be generated in vitro without any cellular cofactors or PrP^{Sc}-dependent templating. To date, the relationship between the novel and classical PrP^{Sc} remains speculative, but the results of proteolytic digestion of PrP^{Sc} carried out under partially denaturing conditions may provide an important link between the two forms (Kocisko et al. 1996). Caughey and coauthors showed that PK treatment of in vivo-derived hamster PrP^{Sc} in the presence of 2.5 M GdnHCl resulted in digestion of the N-terminal regions including residues 90–115 and, possibly, 90–143, while the C-terminal region remained intact (Fig. 3D;Kocisko et al. 1996). The C-terminal fragments of PrP^{Sc} generated under partially denaturing conditions (Kocisko et al. 1996) were similar to those produced from novel PrP^{Sc} under native conditions (Zou et al. 2003). If the classical and novel subpopulations of PrP^{Sc} indeed share a similar substructure, the novel subpopulation may represent a metabolic intermediate or byproduct of formation of classical PrP^{Sc}. Remarkably, the third site targeted by PK in both the amyloid fibrils and the novel subpopulation of PrP^{Sc} (residue 162) coincides with the sequence YYR (residues 162–164) (Paramithiotis et al. 2003). Epitope mapping using antibodies raised to a peptide including this sequence has shown that the epitope containing these residues is buried in the native PrP^{C} form, but becomes solvent-exposed upon conversion to pathological PrP^{Sc} form.

Since the relative proportions of two amyloid conformers generated in vitro are opposite to that of novel and classical PrP^{Sc} in sporadic CJD, as yet unidentified cellular cofactors may be required for efficient conversion of rPrP 23-230 into a conformer similar to classical PrP^{Sc}. Such a cofactor may promote assembly by counteracting the electrostatic repulsion of positively charged N-terminal regions that remain exposed to the solvent upon conversion to the amyloid form. Polyanions such as sulfated glycans or RNA may serve this function. RNA and heparin sulfate have been shown to bind to the N-terminal region of PrP^{C} (Gonzalez-Iglesias et al. 2002; Warner et al. 2002; Gabus et al. 2004) and, furthermore, both RNA and sulfated glycans were found to stimulate cell-free conversion of PrP^{C} into protease-resistant PrP^{Sc}-like forms (Wong et al. 2001; Adler et al. 2003; Deleault et al. 2003).

While the amyloid fibrils formed by rPrP 89-230 were shown to cause a transmissible form of prion disease in experimental animals, the incubation times observed upon inoculation of the fibrils was longer than that exhibited by most known PrP^{Sc} strains (Legname et al. 2004). It is important to note that natural strains of PrP^{Sc} evolved through natural selection (Bartz et al. 2000). Only those strains that show very fast rates of propagation and, correspondingly, shorter incubation times are preferred by many laboratory investigators. Moreover, most strains that are currently used in laboratories were repassaged many times and therefore adapt well to a particular host. One can speculate that the shortening of the incubation times observed in the second passages of synthetic prions may be attributed to the adaptation to the host, suggesting that an apparent transmission barrier precludes efficient propagation of the amyloid fibrils in the first passage. A transmission barrier is typically ob-

served when the sequence of PrP^{Sc} in the inoculum does not match that of PrP^{C} in the recipient animals (Pattison and Jones 1968; Prusiner et al. 1990; Scott et al. 1993). Besides the differences in the sequences of PrPs, different strains of prion disease have different transmission barriers, presumably as a result of different conformations of PrP^{Sc} (Barron et al. 2003). Since the sequence of the amyloid fibrils was identical to that of endogenously expressed PrP^{C} (mouse PrP 89-230), it is likely that the apparent transmission barrier is due to the unique conformational properties of the amyloid fibrils and, in particular, due to the proteolytic liability of residues 90–138. In addition, the lack of glycosylation in the amyloid fibrils may affect their conformational compatibility to PrP^{C} and, therefore, also contribute to the slow rate of propagation in the first passage and the apparent transmission barrier. Remarkably, after primary passage was accomplished, much shorter incubation times in the second passage of the synthetic prions were observed (Legname et al. 2004).

PK resistance of the central region and, in particular, the 3F4 epitope (residues 108–111) has historically been exploited to distinguish PrP^{Sc} from PrP^{C} as a biochemical marker for the presence of prion infection (McKinley et al. 1983; Oesch et al. 1985). Taken together, this study and that by Legname and coauthors demonstrate that the amyloid fibrils generated in vitro are capable of transmitting a prion disease despite having a proteolytically labile region encompassing residues 90–138. These findings may explain reports of prion infections in the absence of detectable PK-resistant PrP^{Sc} (Lasmézas et al. 1997; Manuelidis et al. 1997; Barron et al. 2001; Tremblay et al. 2004). These observations have serious implications for the development of effective prion diagnostics.

Materials and methods

Expression and purification of recombinant PrPs

Mouse rPrP encompassing residues 89–230 was expressed and purified as described previously (Baskakov 2004). The purified proteins were confirmed to be single species with an intact disulfide bond by SDS-PAGE and electrospray mass spectrometry. Detailed protocols for purification and refolding of full-length mouse rPrP 23-230 are described by Bocharova et al. (2005). Briefly, the purification was achieved using NTA Fast Flow Sepharose resin (Amersham Biosciences) precharged with Ni-ions, followed by reverse-phase chromatography on C4 HPLC column (Vydac). rPrP 23-230 was confirmed to be 99.5+% pure with an intact disulfide bond by SDS-PAGE with silver staining, electrospray mass spectrometry, and analytical size-exclusion chromatography.

In vitro conversion of PrPs into the amyloid fibrils

To form amyloid fibrils we used two different formats, manual and automated. In the manual format, a stock solution of rPrP 89-230 or rPrP 23-230 (4 mg/mL) in 6 M GdnHCl was diluted to the final protein concentration of 0.5 mg/mL and incubated at 37°C in 20 mM Na-acetate buffer, 1 M GdnHCl, 3 M urea, 150 mM NaCl (pH 5.0) with continuous shaking at 600 rpm using a Delfia plate shaker (Wallac) in conical plastic tubes (Eppendorf) in a 0.6-mL reaction volume. The kinetics of fibril formation were monitored using a ThT-binding assay. Aliquots withdrawn during the time course of incubation at 37°C were diluted into 5 mM Na-acetate buffer (pH 5.5) to a final concentration of rPrP of 1 μM, and then ThT (Molecular Probes) was added to a final concentration of 10 μM. Six emission spectra (from 460 to 520 nm) were recorded for each sample in 0.4-cm rectangular cuvettes with excitation at 445 nm on a FluoroMax-3 fluorimeter (Jobin Yvon); both excitation and emission slits were 4 nm. Spectra were averaged and the fluorescence intensity at emission maximum (482 nm) was determined. In a typical experiment, we observed a 50-fold increase in ThT-fluorescence per 1 μM of rPrP 89-230 upon conversion into the amyloid form.

To monitor the kinetics of amyloid formation in seeding experiments, we used the automated format. The conversion in the automated format was carried out in PBS buffer, 1 M GdnHCl, 3 M urea (pH 7.0) in a 0.15-mL volume in 96-well plates and in the presence of ThT (10 μM). Our preliminary studies using the manual format demonstrated that the presence of 10 μM ThT in the reaction mixture does not interfere with the kinetics of amyloid formation (data not shown). Three Teflon spheres (2.38-mm diameter, McMaster-Carr) were placed into each well of a 96-well plate; then the reaction mixture containing rPrP and ThT was pipetted into wells, and the plates were covered by ELAS septum sheets (Spike International), and incubated at 37°C upon continuous shaking at 900 rpm in a Fluoroskan Ascent CF microplate reader (ThermoLabsystems). The kinetics were monitored by bottom reading of fluorescence intensity every 5 min using 444 nm excitation and 485 nm emission filters.

The lag phase of amyloid formation was determined by fitting the time-dependent changes in the fluorescence of ThT (F) over time of the reaction (t) to the following equation:

$$F = A + B / (1 + \exp [k^* (t_m - t)]$$

where A is the base level of ThT fluorescence during the lag phase, B is the difference between final level of ThT fluorescence at plateau and the initial level during the lag phase, k is the rate constant of fibril growth (h^{-1}), and t_m is the observed time at midpoint of transition. The lag time (t_l) of fibril formation was calculated as: $t_l = t_m - 2/k$. The apparent seeding activities in the reactions seeded with 2.5% of fibrils pretreated with PK were calculated using the linear dependence between the length of the lag phase and Lg[amount of seed].

GdnHCl-induced denaturation of the amyloid fibrils

Mo rPrP 89-230 in amyloid conformation (7 μL, 0.4 mg/mL) was suspended in PBS (30 μL, pH 7.2) containing GdnHCl (0.5–5.5 M). This solution was incubated for 30 min at a fixed temperature (24°C or 57°C) and then diluted to 300 μL with 8 M GdnHCl and water to adjust the final concentration of GdnHCl to 0.55 M. Fluorescence spectra were recorded in the presence of 10 μM thioflavin T (ThT) in 0.4-cm rectangular cuvettes, with excitation at 445 nm, on a FluoroMax-3 fluorimeter (Jobin Yvon) at 24°C; both excitation and emission slits were 4 nm. ThT bound to the amyloid fibrils showed typical fluorescence spectra with the emission maximum at 482 nm. Background ThT fluorescence was subtracted. $C_{1/2}$ values were calculated according to the equation $C_{1/2} = \Delta G/m$, where ΔG is apparent free energy of denaturation,

and *m* represents the GdnHCl concentration dependence of the free energy of denaturation. ΔG and *m* values were calculated using least-squares fit of the data to a two-state model using the linear extrapolation method as described (Santoro and Bolen 1988).

Proteolysis with proteinase K

The amyloid forms or α-helical forms of rPrP 89-230 (0.2 mg/mL) and rPrP 23-230 (0.2 mg/mL) were dialyzed and treated with PK at 37°C for 1 h in 100 mM Tris-HCl buffer (pH 7.2). Digestion was stopped by quenching with PMSF (2 mM), followed by addition of 8 M urea, to a final concentration of 3 M, and 4X sample buffer to a final concentration of 1X. Samples were heated at 95°C for 5 min and analyzed by SDS-PAGE by use of precast 12% NuPage SDS gels (Invitrogen). For Western blot experiments, proteins were electroblotted onto Immobilon P PVDF membrane (Millipore), incubated with anti-PrP Fabs (0.2 μg/mL) followed by incubation with goat anti-human IgG F(ab)2 fragment conjugated with HRP, and detected using the ECL system (Pierce).

FTIR spectroscopy

FTIR spectra were measured by means of a Bruker Tensor 27 FTIR instrument (Bruker Optics) equipped with an MCT detector cooled with liquid nitrogen. Both α-rPrP and amyloid fibrils were dialyzed against 10 mM Na-acetate buffer (pH 5.5), and 10 μL of each isoform (3 mg/mL of α-rPrP, or 0.3 mg/mL of the amyloid fibrils) was loaded into a BioATRcell II. Then, 128 scans at 2-cm^{-1} resolution were collected for each sample under constant purging with nitrogen, corrected for water vapor; background spectra of buffer were subtracted.

Mass spectrometry

Online capillary LC-MS analyses were performed at the Institute for Animal Health proteomics facility as described (Gill et al. 2000). Briefly, samples were diluted to ~1 pmol/μL in 95:5 H_2O:acetonitrile with 0.05% trifluoroacetic acid (TFA) (solvent A), and ~20 pmol was injected onto a preconcentration trap and desalted by washing with the above solvent. Components were separated on a home-packed capillary HPLC column (180-μm i.d., 5-μm beads, 300 Å pore size, Jupiter C_{18}, Phenomenex), previously equilibrated with solvent A, and were eluted by an increasing gradient of solvent B, where solvent B was 5:95 H_2O:acetonitrile with 0.05% TFA. The flow rate was ~1 μL/min. The column eluent was passed directly to a Quattro II tandem quadrupole mass spectrometer (Waters UK) operated in positive ion mode. The instrument was equipped with a continuous flow nanospray source and acquired full scan mass spectra (m/z 300–2100) every 5 sec.

Negative staining and electron microscopy

Negative staining was performed on carbon-coated 100-mesh grids coated with 0.01% of poly-L-lysine solution prior to staining. The samples were adsorbed for 30 sec, washed with 0.1 M and 0.01 M Na-acetate for 5 sec each, stained with freshly filtered 2% uranyl acetate for 30 sec, dried, and then viewed in a Zeiss EM 10 CA electron microscope.

Epifluorescence microscopy

Epifluorescence microscopy was carried out on an inverted microscope (Nikon Eclipse TE2000-U) with the illumination system X-Cite 120 (EXFO Photonics Solutions) connected through fiber optics using a 1.3 aperture Plan Fluor 100x NA objective. The emission was isolated from Rayleigh and Raman-shifted light by a combination of filters: an excitation filter 485DF22, a beam splitter 505DRLPO2, and an emission filter 510LP (Omega Optical). Digital images were acquired using a cooled 12-bit CoolSnap HQ CCD camera (Photometrics). Fibrils were prestained with ThT (10 μM) for 3 min prior to imaging.

Acknowledgments

This work was supported by NIH grants AG022116 and NS045585 to I.V.B. and by the BBSRC at IAH Compton.

References

Adler, V., Zeiler, B., Kryukov, V., Kascsak, R., Rubenstein, R., and Grossman, A. 2003. Small, highly structured RNAs participate in the conversion of human recombinant PrPsen to PrPres in vitro. *J. Mol. Biol.* **332:** 47–57.

Barron, R.M., Thomson, V., Jameison, E., Melton, D.W., Ironside, J., Will, R., and Manson, J.C. 2001. Changing a single amino acid in the N-terminus of murine PrP alters TSE incubation time across three species barriers. *EMBO J.* **20:** 5070–5078.

Barron, R.M., Thomson, V., King, D., Shaw, J., Melton, D.W., and Manson, J.C. 2003. Transmission of murine scrapie to P101L transgenic mice. *J. Gen. Virol.* **84:** 3165–3172.

Bartz, J.C., Bessen, R.A., McKenzie, D., Marsh, R.F., and Aiken, J.M. 2000. Adaptation and selection of prion protein strain conformations following interspecies transmission of transmissible mink encephalopathy. *J. Virol.* **74:** 5542–5547.

Baskakov, I.V. 2004. Autocatalytic conversion of recombinant prion proteins displays a species barrier. *J. Biol. Chem.* **279:** 586–595.

Baskakov, I.V., Legname, G., Prusiner, S.B., and Cohen, F.E. 2001. Folding of prion protein to its native α-helical conformation is under kinetic control. *J. Biol. Chem.* **276:** 19687–19690.

Baskakov, I.V., Legname, G., Baldwin, M.A., Prusiner, S.B., and Cohen, F.E. 2002. Pathway complexity of prion protein assembly into amyloid. *J. Biol. Chem.* **277:** 21140–21148.

Bessen, R.A. and Marsh, R.F. 1994. Distinct PrP properties suggest the molecular basis of strain variation in transmissible mink encephalopathy. *J. Virol.* **68:** 7859–7868.

Bocharova, O.V., Breydo, L., Parfenov, A.S., Salnikov, V.V., and Baskakov, I.V. 2005. In vitro conversion of full length mammalian prion protein produces amyloid form with physical property of PrPSc. *J. Mol. Biol.* **346:** 645–659.

Caughey, B.W., Dong, A., Bhat, K.S., Ernst, D., Hayes, S.F., and Caughey, W.S. 1991. Secondary structure analysis of the scrapie-associated protein PrP 27-30 in water by infrared spectroscopy. *Biochemistry* **30:** 7672–7680.

Caughey, B., Raymond, G.J., and Bessen, R.A. 1998. Strain-dependent differences in β-sheet conformations of abnormal prion protein. *J. Biol. Chem.* **273:** 32230–32235.

Chabry, J., Caughey, B., and Chesebro, B. 1998. Specific inhibition of in vitro formation of proteinase-resistant prion protein by synthetic peptides. *J. Biol. Chem.* **273:** 13203–13207.

Chen, S.G., Teplow, D.B., Parchi, P., Teller, J.K., Gambetti, P., and Autilio-Gambetti, L. 1995. Truncated forms of the human prion protein in normal brain and in prion diseases. *J. Biol. Chem.* **270:** 19173–19180.

Cohen, F.E., Pan, K.-M., Huang, Z., Baldwin, M., Fletterick, R.J., and Prusiner, S.B. 1994. Structural clues to prion replication. *Science* **264:** 530–531.

Deleault, N.R., Lucassen, R.W., and Supattapone, S. 2003. RNA molecules stimulate prion protein conversion. *Nature* **425:** 717–720.

Dickinson, A.G., Meikle, V.M.H., and Fraser, H. 1968. Identification of a gene which controls the incubation period of some strains of scrapie agent in mice. *J. Comp. Pathol.* **78:** 293–299.

Donne, D.G., Viles, J.H., Groth, D., Mehlhorn, I., James, T.L., Cohen, F.E., Prusiner, S.B., Wright, P.E., and Dyson, H.J. 1997. Structure of the recom-

binant full-length hamster prion protein PrP(29-231): The N terminus is highly flexible. *Proc. Natl. Acad. Sci.* **94:** 13452–13457.
Fischer, M., Rülicke, T., Raeber, A., Sailer, A., Moser, M., Oesch, B., Brandner, S., Aguzzi, A., and Weissmann, C. 1996. Prion protein (PrP) with amino-proximal deletions restoring susceptibility of PrP knockout mice to scrapie. *EMBO J.* **15:** 1255–1264.
Fraser, H. and Dickinson, A.G. 1973. Scrapie in mice. Agent-strain differences in the distribution and intensity of grey matter vacuolation. *J. Comp. Pathol.* **83:** 29–40.
Gabizon, R. and Prusiner, S.B. 1990. Prion liposomes. *Biochem. J.* **266:** 1–14.
Gabus, C., Derrington, E., Leblanc, P., Chnaiderman, J., Dormont, D., Swietnicki, W., Morillas, M., Surewicz, W.K., Marc, D., Nandi, P., et al. 2004. The prion protein has RNA binding chaperoning properties characteristic of nucleocasid protein NCP7 of HIV-1. *J. Biol. Chem.* **276:** 19301–19309.
Gill, A.C., Ritchie, M.A., Hunt, L.G., Steane, S.E., Davies, K.G., Bocking, S.P., Rhie, A.G., Bennett, A.D., and Hope, J. 2000. Post-translational hydroxylation at the N-terminus of the prion protein reveals presence of PPII structure in vivo. *EMBO J.* **19:** 5324–5331.
Gonzalez-Iglesias, R., Pajares, M.A., Espinosa, C.O.J.C., Oesch, B., and Gasset, M. 2002. Prion protein interaction with glycosaminoglycan occurs with the formation of oligomeric complexes stabilized by Cu(II) bridges. *J. Mol. Biol.* **319:** 527–540.
Haire, L.F., Whyte, S.M., Vasisht, N., Gill, A.C., Verma, C., Dodson, E.J., Dodson, G.G., and Bayley, P.M. 2004. The crystal structure of the globular domain of sheep prion protein. *J. Mol. Biol.* **336:** 1175–1183.
Hill, A.F., Joiner, S., Wadsworth, J.D.F., Sidle, K.C.L., Bell, J.E., Budka, H., Ironside, J.W., and Collinge, J. 2003. Molecular classification of sporadic Creutzfeldt-Jakob disease. *Brain* **126:** 1333–1346.
Kocisko, D.A., Lansbury Jr., P.T., and Caughey, B. 1996. Partial unfolding and refolding of scrapie-associated prion protein: Evidence for a critical 16-kDa C-terminal domain. *Biochemistry* **35:** 13434–13442.
Lasmézas, C.I., Deslys, J.-P., Robain, O., Jaegly, A., Beringue, V., Peyrin, J.-M., Fournier, J.-G., Hauw, J.-J., Rossier, J., and Dormont, D. 1997. Transmission of the BSE agent to mice in the absence of detectable abnormal prion protein. *Science* **275:** 402–405.
Lawson, V.A., Priola, S.A., Meade-White, K., Lawton, M., and Chesebro, B. 2004. Flexible N-terminal region of prion protein influences conformation of protease resistant prion protein isoforms associated with cross-species scrapie infection in vivo and in vitro. *J. Biol. Chem.* **279:** 13689–13695.
Legname, G., Baskakov, I.V., Nguyen, H.-O.B., Riesner, D., Cohen, F.E., DeArmond, S.J., and Prusiner, S.B. 2004. Synthetic mammalian prions. *Science* **305:** 673–676.
Legname, G., Nguyen, H.-O.B., Baskakov, I.V., Cohen, F.E., DeArmond, S.J., and Prusiner, S.B. 2005. Strain-specified characteristics of mouse synthetic prions. *Proc. Natl. Acad. Sci.* **102:** 2168–2173.
Manuelidis, L., Fritch, W., and Xi, Y.-G. 1997. Evolution of a strain of CJD that induces BSE-like plaques. *Science* **277:** 94–98.
McKinley, M.P., Bolton, D.C., and Prusiner, S.B. 1983. A protease-resistant protein is a structural component of the scrapie prion. *Cell* **35:** 57–62.
Notari, S., Capellari, S., Giese, A., Westner, I., Baruzzi, A., Ghetti, B., Gambetti, P., Kretzschmar, H.A., and Parchi, P. 2004. Effects of different experimental conditions on the PrPSc core generated by protease digestion. *J. Biol. Chem.* **279:** 16797–16804.
Oesch, B., Westaway, D., Wälchli, M., McKinley, M.P., Kent, S.B.H., Aebersold, R., Barry, R.A., Tempst, P., Teplow, D.B., Hood, L.E., et al. 1985. A cellular gene encodes scrapie PrP 27-30 protein. *Cell* **40:** 735–746.
Pan, K.-M., Baldwin, M., Nguyen, J., Gasset, M., Serban, A., Groth, D., Mehlhorn, I., Huang, Z., Fletterick, R.J., Cohen, F.E., et al. 1993. Conversion of α-helices into β-sheets features in the formation of the scrapie prion proteins. *Proc. Natl. Acad. Sci.* **90:** 10962–10966.
Paramithiotis, E., Pinard, M., Lawton, T., LaBoissiere, S., Leathers, V.L., Zou, W.Q., Estey, L.A., Lamontagne, J., Lehto, M.T., Kondejewski, L.H., et al. 2003. A prion protein epitope selective for the pathologically misfolded conformation. *Nat. Med.* **9:** 893–899.
Parchi, P., Giese, A., Capellari, S., Brown, P., Schulz-Schaeffer, W., Windl, O., Zerr, I., Budka, H., Kopp, N., Piccardo, P., et al. 1999. Classification of sporadic Creutzfeldt-Jakob disease based on molecular and phenotypic analysis of 300 subjects. *Ann. Neurol.* **46:** 224–233.
Parchi, P., Zou, W., Wang, W., Brown, P., Capellari, S., Ghetti, B., Kopp, N., Schulz-Schaeffer, W.J., Kretzschmar, H.A., Head, M.W., et al. 2000. Genetic influence on the structural variations of the abnormal prion protein. *Proc. Natl. Acad. Sci.* **97:** 10168–10172.
Pattison, I.H. and Jones, K.M. 1968. Modification of a strain of mouse-adapted scrapie by passage through rats. *Res. Vet. Sci.* **9:** 408–410.
Peretz, D., Williamson, R.A., Matsunaga, Y., Serban, H., Pinilla, C., Bastidas, R.B., Rozenshteyn, R., James, T.L., Houghten, R.A., Cohen, F.E., et al. 1997. A conformational transition at the N terminus of the prion protein features in formation of the scrapie isoform. *J. Mol. Biol.* **273:** 614–622.
Peretz, D., Scott, M., Groth, D., Williamson, A., Burton, D., Cohen, F.E., and Prusiner, S.B. 2001. Strain-specified relative conformational stability of the scrapie prion protein. *Protein Sci.* **10:** 854–863.
Prusiner, S.B. 1982. Novel proteinaceous infectious particles cause scrapie. *Science* **216:** 136–144.
———. 2001. Shattuck lecture—Neurodegenerative diseases and prions. *N. Engl. J. Med.* **344:** 1516–1526.
Prusiner, S.B., Scott, M., Foster, D., Pan, K.-M., Groth, D., Mirenda, C., Torchia, M., Yang, S.-L., Serban, D., Carlson, G.A., et al. 1990. Transgenetic studies implicate interactions between homologous PrP isoforms in scrapie prion replication. *Cell* **63:** 673–686.
Prusiner, S.B., Groth, D., Serban, A., Stahl, N., and Gabizon, R. 1993. Attempts to restore scrapie prion infectivity after exposure to protein denaturants. *Proc. Natl. Acad. Sci.* **90:** 2793–2797.
Riek, R., Hornemann, S., Wider, G., Billeter, M., Glockshuber, R., and Wüthrich, K. 1996. NMR structure of the mouse prion protein domain PrP(121-231). *Nature* **382:** 180–182.
Riek, R., Hornemann, S., Wider, G., Glockshuber, R., and Wüthrich, K. 1997. NMR characterization of the full-length recombinant murine prion protein, *m*PrP(23–231). *FEBS Lett.* **413:** 282–288.
Safar, J., Wille, H., Itri, V., Groth, D., Serban, H., Torchia, M., Cohen, F.E., and Prusiner, S.B. 1998. Eight prion strains have PrP^{Sc} molecules with different conformations. *Nat. Med.* **4:** 1157–1165.
Santoro, M.M. and Bolen, D.W. 1988. Unfolding free energy changes determined by the linear extrapolation method. 1. Unfolding of phenylmethanesulfonyl α-chymotrypsin using different denaturants. *Biochemistry* **27:** 8063–8068.
Satoh, K., Muramoto, T., Tanaka, T., Kitamoto, N., Ironside, J.W., Nagashima, K., Yamada, M., Sato, T., Mohri, S., and Kitamoto, T. 2003. Association of an 11–12 kDa protease-resistant prion protein fragment with subtypes of dura graft-associated Creutzfeldt-Jakob disease and other prion diseases. *J. Gen. Virol.* **84:** 2885–2893.
Scott, M., Groth, D., Foster, D., Torchia, M., Yang, S.-L., DeArmond, S.J., and Prusiner, S.B. 1993. Propagation of prions with artificial properties in transgenic mice expressing chimeric PrP genes. *Cell* **73:** 979–988.
Swietnicki, W., Petersen, R.B., Gambetti, P., and Surewicz, W.K. 1998. Familial mutations and the thermodynamic stability of the recombinant human prion protein. *J. Biol. Chem.* **273:** 31048–31052.
Tagliavini, F., Prelli, F., Verga, L., Giaccone, G., Sarma, R., Gorevic, P., Ghetti, B., Passerini, F., Ghibaudi, E., Forloni, G., et al. 1993. Synthetic peptides homologous to prion protein residues 106–147 form amyloid-like fibrils in vitro. *Proc. Natl. Acad. Sci.* **90:** 9678–9682.
Telling, G.C., Scott, M., Mastrianni, J., Gabizon, R., Torchia, M., Cohen, F.E., DeArmond, S.J., and Prusiner, S.B. 1995. Prion propagation in mice expressing human and chimeric PrP transgenes implicates the interaction of cellular PrP with another protein. *Cell* **83:** 79–90.
Telling, G.C., Parchi, P., DeArmond, S.J., Cortelli, P., Montagna, P., Gabizon, R., Mastrianni, J., Lugaresi, E., Gambetti, P., and Prusiner, S.B. 1996. Evidence for the conformation of the pathologic isoform of the prion protein enciphering and propagating prion diversity. *Science* **274:** 2079–2082.
Tremblay, P., Ball, H.L., Kaneko, K., Groth, D., Hegde, R.S., Cohen, F.E., DeArmond, S., Prusiner, S.B., and Safar, J. 2004. Mutant PrPSc conformers induced by a synthetic peptide and several prion strains. *J. Virol.* **78:** 2088–2099.
Wadsworth, J.D.F., Hill, A.F., Joiner, S., Jackson, G.S., Clarke, A.R., and Collinge, J. 1999. Strain-specific prion-protein conformation determined by metal ions. *Nat. Cell Biol.* **1:** 55–59.
Warner, R.G., Hundt, C., Weiss, S., and Turnbull, J.E. 2002. Identification of the heparan sulfate binding sites in the cellular prion protein. *J. Biol. Chem.* **277:** 18421–18430.
Wille, H., Michelitsch, M.D., Guenebaut, V., Supattapone, S., Serban, A., Cohen, F.E., Agard, D.A., and Prusiner, S.B. 2002. Structural studies of the scrapie prion protein by electron crystallography. *Proc. Natl. Acad. Sci.* **99:** 3563–3568.
Wong, C., Xiong, L.W., Horiuchi, M., Raymond, L., Wehrly, K., Chesebro, B., and Caughey, B. 2001. Sulfated glycans and elevated temperature stimulate PrP(Sc)-dependent cell-free formation of protease-resistant prion protein. *EMBO J.* **20:** 377–386.
Yadavalli, R., Guttmann, R.P., Seward, T., Centers, A.P., Williamson, R.A., and Telling, G.C. 2004. Calpain-dependent endoproteolytic cleavage of PrPSc modulates scrapie prion. *J. Biol. Chem.* **279:** 21948–21956.
Zou, W.Q., Capellari, S., Parchi, P., Sy, M.S., Gambetti, P., and Chen, S.G. 2003. Identification of novel proteinase K-resistant C-terminal fragments of PrP in Creutzfeldt-Jakob disease. *J. Biol. Chem.* **278:** 40429–40436.